

Ground Effect on Aerodynamic Characteristics of Flapping-Wing Micro Air Vehicles

Anh-Tuan Nguyen^{1*}, Thanh-Trung Vu¹, Thanh-Dong Pham¹, Cong-Truong Dinh²

¹Le Quy Don Technical University - No. 236, Hoang Quoc Viet Street, Bac Tu Liem District, Ha Noi, Viet Nam

²Hanoi University of Science and Technology - No. 1, Dai Co Viet, Hai Ba Trung, Ha Noi, Viet Nam

Received: December 03, 2019; Accepted: June 22, 2020

Abstract

This paper presents the ground effect on the aerodynamic performance of a hawkmoth-like flapping-wing micro air vehicle. An unsteady aerodynamic model based on the potential-flow theory is used to determine the ground effect at several flight conditions. In this research, the program is written in FORTRAN programming language by using OpenMP library for parallel computing. It was found that the ground effect is the most significant when the flapping-wing micro air vehicle is hovering with a reduction in the lift force when the distance from the center of mass of the flapping-wing micro air vehicle to the ground is below 0.05m. For forward flight, this effect tends to decrease as the flight speed increases.

Keywords: flapping-wing, unsteady aerodynamics, ground effect.

1. Introduction

FWMAVs (flapping-wing micro air vehicles) are normally designed based on the morphology and the flying mechanism of actual insects. In fact, the characteristics of insect flight have been optimized through millions of years of the natural selection process [1]. Compared to other types of aircraft, one of the most noticeable advantages of insect-like FWMAV is the ability to hover and maneuver in many environment conditions. There have been a number of studies on the aerodynamic characteristics of insect-like FWMAV [2-3], however, the influence of the ground effect has not been considered carefully. Some authors have shown several characteristics of the ground effect of insect flight when hovering [4]. However, this phenomenon in forward flight has not been mentioned.

Within the scope of this study, we focus on the simulation and analysis of the ground effect on the aerodynamic characteristics of an insect-like FWMAV while hovering and in forward flight. The unsteady aerodynamics of the flapping-wings is simulated through the panel method written in FORTRAN language using parallel computing. The ground effect is included in the code through the mirror image method. In this paper, the model of the FWMAV is designed based on the geometric and kinematic parameters of the hawkmoth *Manduca sexta*. The body and each wing weigh 1485.0 and 46.87 mg, respectively; the wing length is 48.5 mm. Here, we use four coordinate systems, including the

ground-fixed, the body-fixed and the two wing-fixed coordinated systems as shown in Fig. 1. In this figure, β is an angle between the stroke plane of the wings and the body axis. The wing orientations are defined by three Euler angles as shown in Fig.2.

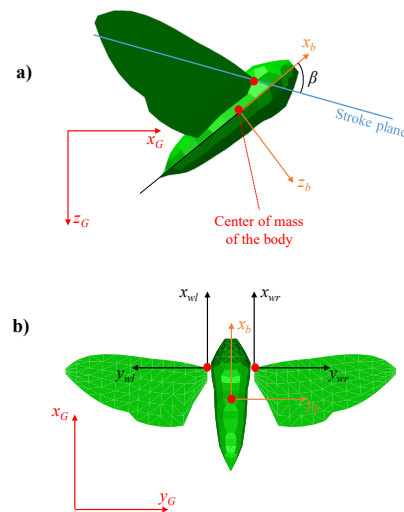


Fig. 1. The FWMAV model and the coordinate systems used in this study

2. Research method

2.1. Panel method

The panel method is based on the potential flow theory [5], which is applied to low-speed and inviscid flows. According to this method, the surface of the FWMAV is divided into aerodynamic panels (Fig.3), on which we place the sources and doublets with constant strength. The velocity potential of the flow is

*Corresponding author: Tel.: (+84) 88000438
Email: anhtuanguyen2410@gmail.com.

the sum of those generated by the sources, doublets on the surface of the FWMAV and the wake:

$$\Phi(\mathbf{r}, t) = -\frac{1}{4\pi} \int_{S_{bd}} \left[\sigma \left(\frac{1}{r} \right) - \mu \mathbf{n} \cdot \nabla \left(\frac{1}{r} \right) \right] dS + \frac{1}{4\pi} \int_{S_{wk}} \mu \mathbf{n} \cdot \nabla \left(\frac{1}{r} \right) dS \quad (1)$$

where σ and μ are the source and doublet strength; S_{bd} and S_{wk} represent the surfaces of the FWMAV and the wake, respectively.

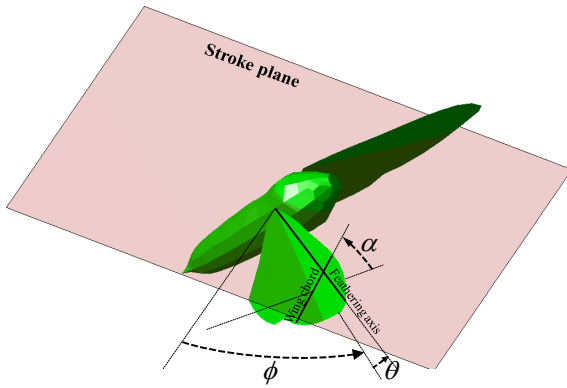


Fig. 2. Euler angles to define the wing orientation

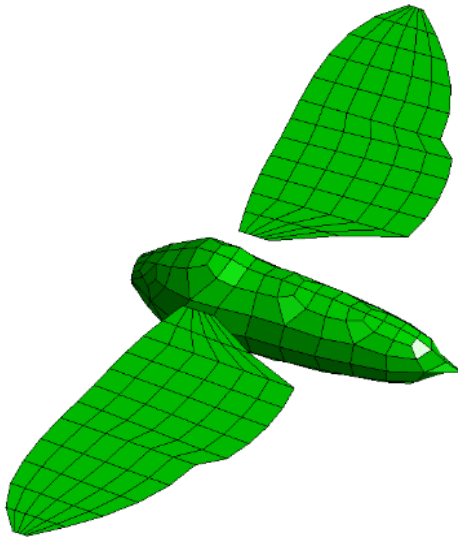


Fig. 3. The mesh on the insect-like FWMAV

Three boundary conditions are considered here, including:

- The far-field boundary condition: at a large distance from the FWMAV the disturbance can be neglected.
- The Neumann boundary condition (no-penetration condition): The relative velocity of the

flow on the object surface is parallel to the surface. This condition is used to determine the source strength.

- The Dirichelet boundary condition: The velocity potential inside the FWMAV body is a constant.

Applying these boundary conditions, we can determine the strength of the sources and doublets [5]. The pressure on the wing and body surfaces of the FWMAV can be calculated by the unsteady Bernoulli equation as follows:

$$p_{bd} = p_{ref} - \rho \left[\frac{1}{2} (\nabla \Phi)^2 - \mathbf{V}_{ref} \cdot \nabla \Phi + \frac{\partial \Phi}{\partial t} \right] \quad (2)$$

To verify the panel method, we compare results with those by a high-order CFD (computational Fluid Dynamics) method for a hawkmoth model (Figure 4).

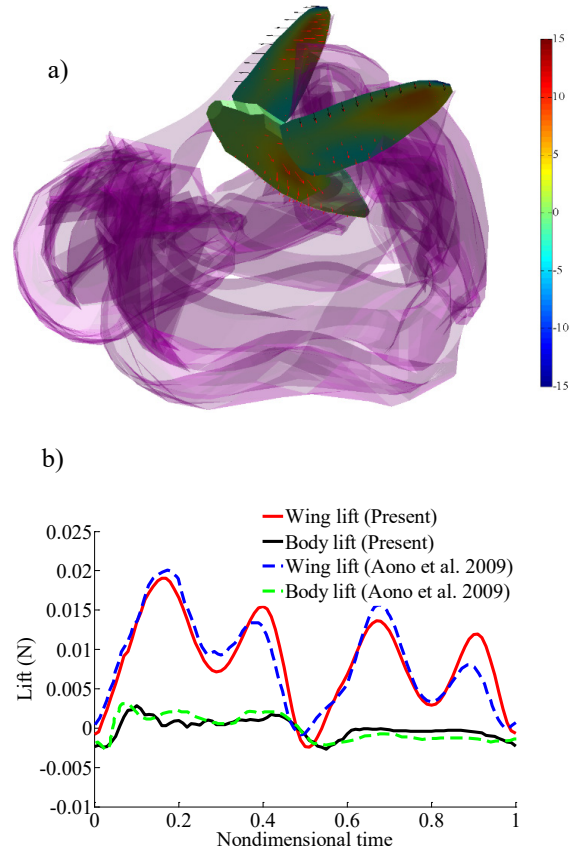


Fig. 4. Pressure distribution on the wing surface by the panel method (a), lift force on the body and wing by the panel and CFD methods [3] (b)

2.2. Mirror image method

The simulation of ground effect is fulfilled by the mirror image method [5] (Figure 5).

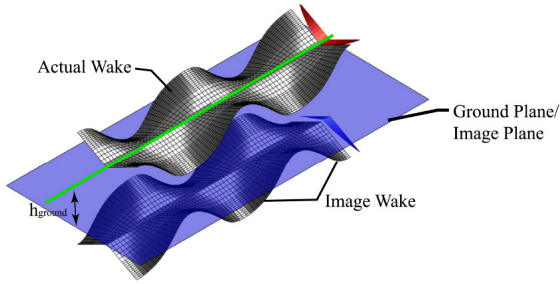


Fig. 5. Simulation of ground effect through the mirror image method

To verify the mirror image method, the lift force coefficient of a robot wing model [4] (figure 6) in ground effect is compared with experimental results. Here, the wing kinematics and the Reynolds number of the robotic wing model are similar to those of a biological hawkmoth wing. The mean wing-tip velocity is used as a reference velocity to define the lift force coefficient C_L .

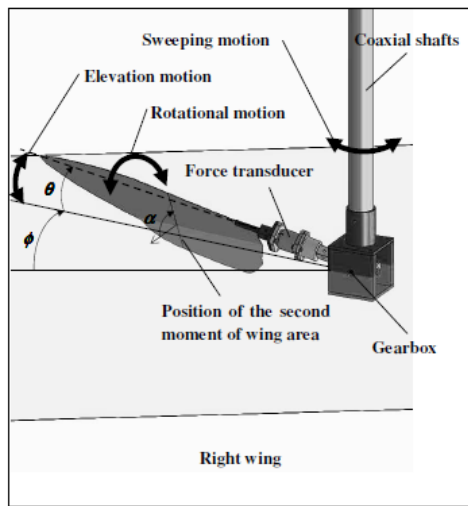


Fig. 6. Hawkmoth-like robot wing model.

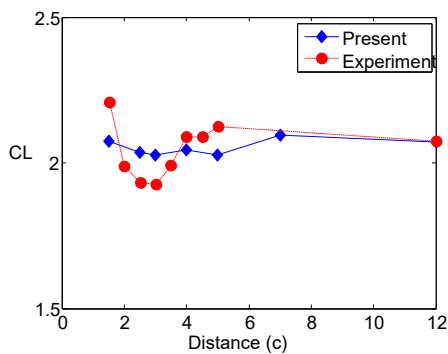


Fig. 7. The lift coefficient C_L from the panel method and an experiment

Figure 7 shows the comparison results. In this figure, the horizontal axis represents the distance from the robot to the ground normalized by the mean chord of the wing c . We can see that although there are some differences when flying near the ground, the simulation method based on mirror image reflection basically has the very similar results to those from the experiment. At a distance from 1.5 to about 6.0 times of the mean chord, the ground effect is quite complicated. In this region, the lift force experiences a decline that is followed by an increase before reaching a steady value at a distance of approximately 6.0 times of the mean chord.

3. Calculation of the ground effect influenced to the lift force parameters of the hawkmoth model

3.1. Calculation of the ground effect in hover

Figure 8 shows the results when calculating the lift force during the fifth and sixth flapping periods of the insect-like FWMAV. It can be seen that at the first half of each period (the upstroke period), no noticeable difference in the lift force is seen when changing the distance from $h = 0.03$ m to 0.06 m. However, in the second half (the downstroke), the difference becomes clearer.

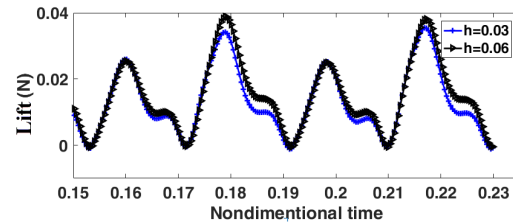


Fig. 8. Comparison of lift forces in cases of flying distance from ground is 0.03 m and 0.06 m

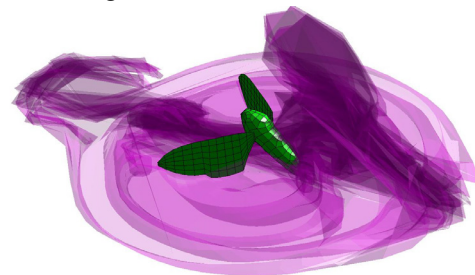


Fig. 9. Vortex field around flapping wing

Surprisingly, unlike fixed-wing aircraft, the ground effect in hover reduces the lift force. This trend can be explained by the presence of strong vortices that shed from the wings after each half stroke. These vortices initially move downward to collide into the ground and then bounce back (Figure 9). When the wings move backward and impinge on these vortices in the next half stroke, the lift force declines. For fixed-wing aircraft, the wing-vortex impingement does not occur; hence, the lift reduction

effect is not observed. Instead, the lift force increases due to the air-cushion effect.

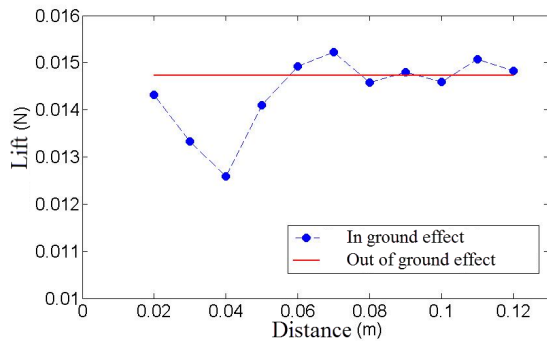


Fig. 10. The average lift change by distance to the ground

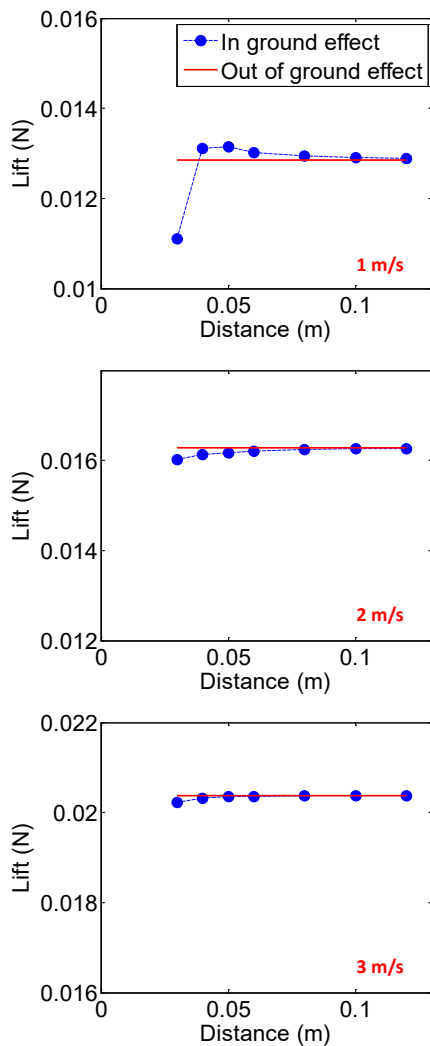


Fig. 11. Ground effect at different speeds

The average lift force variation in the sixth period against the distance to the ground is shown in Figure 10.

Obviously, at a distance to the ground below 0.05 m, the ground effect reduces the average lift force. At a larger distance, the trend of the lift force follows that of fixed-wing aircraft, which means this force decreases when the distance is enlarged.

3.2. Calculation of ground effect in case of forward flight

According to Figure 11, it is seen that the ground effect decreases as the forward speed increases. From 2 m/s, the role of the ground effect is negligible. However, at a velocity value of 1 m/s, this effect is still large.

Figure 12 illustrates the time histories of the lift force at the fourth period at 3 m/s. It can be seen that the distance seems to have a very small influence on the result; rather the ground effect is inconsiderable.

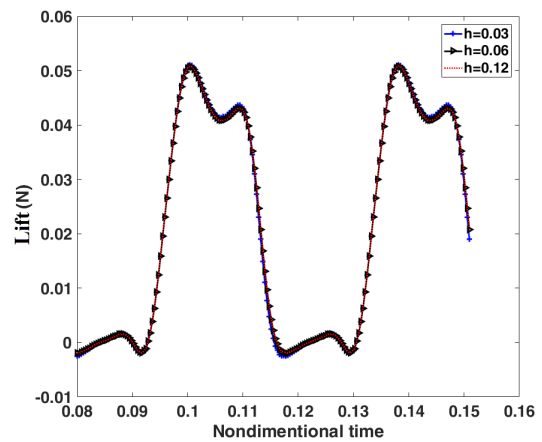


Fig. 12. Ground effect on the lift force at 3 m/s

At high speeds, the ground effect is significantly reduced. In these cases, the shed vortices are left behind and no longer affect the wings of the FWMAV. Hence, the ground effect is barely observed.

4. Conclusions

This paper presented the research result on the ground effect of an insect-like FWMAV based on the panel and the mirror image methods. It was shown that when the FWMAV hovers near the ground, the ground effect causes a reduction in the lift force, which is explained by the impingement between the shed vortices and the wings. This reduction can be observed when the distance from the center of mass of the FWMAV to the ground is below 0.05 m. When the FWMAV moves forward at a high speed, the ground effect is minimal. However, at low-speed flight (1 m/s), this effect is still considerable and has the same trend as the hovering case.

Acknowledgments

This research is funded by Vietnam National Foundation for Science and Technology Development (NAFOSTED) under grant number 107.01-2018.05.

References

- [1] C. P. Ellington. Aerodynamics and the origin of insect flight. *Advances in Insect Physiology*, 23, (1991), pp. 171-210.
- [2] H. Liu, S. Ravi, D. Kolomenskiy, H. Tanaka. Biomechanics and Biomimetics in Insect-Inspired Flight Systems. *Philosophical Transactions B*, 371, (1704), (2016), p. 20150390.
- [3] H. Aono, W. Shyy, H. Liu. Near Wake Vortex Dynamics of a Hovering Hawkmoth. *Acta Mechanica Sinica*, 25, (1), (2009), pp. 23-36.
- [4] X. Zhang, K. B. Lua, R. Chang, T. T. Lim, K. S. Yeo. Experimental Study of Ground Effect on Three-Dimensional Insect-Like Flapping Motion. In 5th International Symposium on Physics of Fluids, (2014), p. 1460384.
- [5] J. Katz, A. Plotkin, *Low-Speed Aerodynamics: From Wing Theory to Panel Methods*, Cambridge University Press, New York (2001).
- [6] A. P. Willmott, C. P. Ellington. The mechanics of flight in the hawkmoth *Manduca sexta*. I. Kinematics of hovering and forward flight. *Journal of Experimental Biology*, 200, (21), (1997), pp. 2705-2722.